Nonlinear Dyn (2014) 76:1469–1484
DOI 10.1007/s11071-013-1221-0

ORIGINAL PAPER

State feedback control at Hopf bifurcation in an exponential RED algorithm model

Min Xiao · Guoping Jiang · Lindu Zhao

Received: 24 January 2013 / Accepted: 20 December 2013 / Published online: 7 January 2014

Abstract In this paper, we show that a state feedback method, which has successfully been used to control unstable steady states or periodic orbits, provides a tool to control the Hopf bifurcation for a novel congestion control model, i.e., the exponential RED algorithm with a single link and single source. We choose the gain parameter as the bifurcation parameter. Without control, the bifurcation will occur early; meanwhile, the model can maintain a stationary sending rate only in a certain domain of the gain parameter. However, outside of this domain the model still possesses a stable sending rate that can be guaranteed by the state feedback control, and the onset of the undesirable Hopf bifurcation is postponed. Numerical simulations are given to justify the validity of the state feedback controller in the bifurcation control.

Keywords Congestion control · Exponential RED · Hopf bifurcation · State feedback · Bifurcation control

M. Xiao (✉) · G. Jiang
College of Automation, Nanjing University of Posts and Telecommunications, Nanjing 210003, China
e-mail: candymanxm2003@aliyun.com

M. Xiao · L. Zhao
School of Economics & Management, Southeast University, Nanjing 210096, China

M. Xiao
School of Mathematics and Information Technology, Nanjing Xiaozhuang University, Nanjing 210017, China

1 Introduction

In the past decades, we have witnessed a rapidly growing interest of bifurcation control due to its promising potential applications in various areas [1]: the prevention of voltage collapse in electric power systems, the stabilization of rotating stall and surge in axial flow compressors, the regulation of human heart rhythms and neuronal activity behavior, the elimination of seizing activities in human cerebral cortex, and so on. In general, bifurcation control refers to the control of bifurcation properties of nonlinear dynamic systems, thereby resulting in some desired output behaviors of the systems, such as delaying the onset of an inherent bifurcation, stabilizing an unstable bifurcated solution or branch, and changing the critical values of an existing bifurcation [2]. Various bifurcation control approaches have been proposed in the literature [3–10]. Particularly, for the problem of relocating an inherent Hopf bifurcation, a dynamic state feedback control law incorporating a washout filter was proposed [3]. Later, the state feedback scheme was successfully developed to control Hopf bifurcations of autonomous systems [6,10]. However, much less is known in the case of applying the state feedback to control bifurcations arising from time-delayed systems. In this paper, the state feedback is adopted to control Hopf bifurcations of a time-delayed congestion control model.

Internet congestion control is an algorithm to regulate the sending rates of the sources such that high network utilization, small amounts of queuing delay,

and some degree of fairness among users are obtained, so as to avoid congestion collapse. The whole Internet congestion and avoidance mechanism is a combination of the end-to-end TCP congestion control mechanism [11,12] at the end hosts and the queue management mechanism at the routers. The basis of TCP congestion control lies in the Additive Increase Multiplicative Decrease (AIMD) mechanism that halves the congestion window for every window containing a packet loss, and increases the congestion window by roughly one segment per round trip time (RTT) otherwise [13]. The queue management mechanism is meant to control the congestion level at each router through different kinds of Active Queue Management (AQM) mechanisms, e.g., Drop Tail [12], Random Early Detection (RED) [14], Random Early Marking (REM) [15], Virtual Queue (VQ) [16], and Adaptive Virtual Queue (AVQ) [17]. The stability, bifurcation, and control of the congestion control algorithm in the Internet have been the focus of intense research in the last few years [18–31].

The exponential RED algorithm model with a single link and single source can be described by

$$\begin{aligned} \dot{x}(t) &= x(t-\tau)\left[\tfrac{1-p(t)}{\tau^2 x(t)} - kx(t)p(t)\right], \\ \dot{p}(t) &= \tfrac{\beta}{c}p(t)(x(t-\tau)-c), \end{aligned} \tag{1}$$

where $x(t)$ is the sending rate of the source, $p(t)$ is the loss probability function, $\tau > 0$ is the RTT, $k > 0$ is a decay factor, $c > 0$ is the link capacity, and $\beta > 0$ is a gain parameter. It is easy to see that system (1) involves delay-dependent parameters, which make the analysis more complex.

In the past few years, many authors have studied system (1) on the bifurcation and control [24,26,28]. By means of the delay τ [24] or gain parameter β [28] as the bifurcation parameter, the stability and Hopf bifurcation were investigated for system (1). It was found that when the delay τ or gain parameter β exceeds a critical value, the congestion control system (1) may lose its stability and undergo a Hopf bifurcation, that is to say, the stationary sending rate cannot be guaranteed, which is not desirable. Thus, the study of bifurcation control for congestion control systems is of significance. A time-delayed feedback scheme was applied to control the Hopf bifurcation for system (1). It was shown that under the control, one can postpone the undesirable onset of the critical value of the delay τ and thus insure a stationary data sending rate for a larger delay.

Although the control of bifurcation has already been discussed in various congestion control systems [19,20,23,26,30], the control schemes used in these literatures are all the time-delayed feedback. The delayed feedback law may have some potential disadvantages such as requiring quite a lot of knowledge about the system state some time ago and making the dynamics take place in infinite-dimensional phase spaces. Therefore, it is needed to design a new control law that can achieve the goal of bifurcation control. In this paper, we will propose a state feedback scheme to control the Hopf bifurcation for system (1). It will be shown that the state feedback controller can increase the critical value of the Hopf bifurcation of the gain parameter β, thereby guaranteeing a stationary sending rate for large gain parameter values.

The rest of the paper is organized as follows. In the next section, the main results for the Hopf bifurcation of model (1) obtained in [28] are summarized. In Sect. 3, we will introduce the bifurcation control for model (1) under the state feedback control. To verify the theoretical analysis, numerical simulations are carried out for an example in Sect. 4. The paper is finished by conclusions presented in Sect. 5.

2 Stability and bifurcation of uncontrolled system (1)

In this section, the results of the stability and Hopf bifurcation for system (1), obtained in [28], are summarized here.

System (1) has a non-zero equilibrium $E^*(x^*, p^*)$, where

$$x^* = c,\ p^* = \frac{1}{1+kc^2\tau^2}. \tag{2}$$

Remark 1 p^* explicitly depends on the delay τ, which makes the analysis about the equilibrium $E^*(x^*, p^*)$ not trivial.

Theorem 1 ([28]) *For each fixed $\tau > 0$, the non-zero equilibrium $E^*(x^*, p^*)$ of system (1) is asymptotically stable when $\beta \in (0, \beta_0)$, and unstable when $\beta > \beta_0$.*

Here,

$$\beta_0 = c\tau^2\sqrt{\omega_0^4 + \left(\frac{2kc}{1+kc^2\tau^2}\right)^2\omega_0^2}, \tag{3}$$

and

$$\omega_0 \in \left(0, \frac{\pi}{2\tau}\right) \tag{4}$$

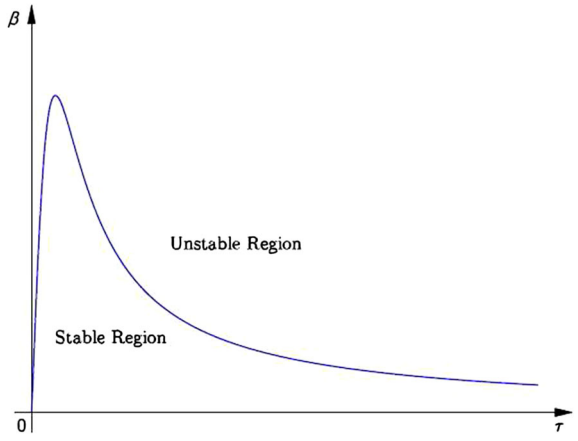

Fig. 1 The curve of β_0 depending on τ divides the first quadrant of (τ, β)-plane into two regions: linear stable region and unstable region. This is Fig. 2 in Hu and Huang [28]

is the root of the equation

$$\frac{1}{\frac{2kc}{1+kc^2\tau^2}}\omega = \cot(\omega\tau). \tag{5}$$

Figure 1 is the bifurcation curve in the parameter plane (τ, β).

Theorem 2 ([28]) *For system (1), a Hopf bifurcation occurs from its non-zero equilibrium, E^*, when the gain parameter, β, passes through the critical value, β_0, where β_0 is defined by (3)–(5).*

Theorem 3 ([28]) *The Hopf bifurcation in the exponential RED algorithm model (1) is determined by the parameters μ_2, ν_2, T_2, where μ_2 determines the direction of the Hopf bifurcation: if $\mu_2 > 0$ ($\mu_2 < 0$), then the Hopf bifurcation is supercritical (subcritical) and the bifurcating periodic solutions exist for $\beta > \beta_0$ ($\beta < \beta_0$); ν_2 determines the stability of the bifurcating periodic solutions: the bifurcating periodic solutions are stable (unstable) if $\nu_2 < 0$ ($\nu_2 > 0$); and T_2 determines the period of the bifurcating periodic solutions: the period increases (decreases) if $T_2 > 0$ ($T_2 < 0$).*

The parameters μ_2, ν_2, T_2 are given by

$$\begin{aligned} c_1(0) &= \frac{i}{2\omega_0}\left(g_{11}g_{20} - 2|g_{11}|^2 - \frac{|g_{02}|^2}{3}\right) + \frac{g_{21}}{2}, \\ \mu_2 &= -\frac{Re\{c_1(0)\}}{Re\{\lambda'(\beta_0)\}}, \\ \nu_2 &= 2Re\{c_1(0)\}, \\ T_2 &= -\frac{Im\{c_1(0)\} + \mu_2 Im\{\lambda'(\beta_0)\}}{\omega_0}. \end{aligned} \tag{6}$$

The detailed derivation of the above formulas can be found in Sect. 3 in [28].

3 Control by state feedback

Many researchers have designed the various time-delayed feedback schemes to control the Hopf bifurcation in the Internet congestion control models [19,20,23,26,30]. However, the time-delayed feedback approach requires quite a lot of knowledge about the system state some time ago, which is not always straightforward to find in a real-life situation. On the other hand, a deep theoretical analysis of such control approach is a formidable task since the time delay causes the corresponding phase space to become infinitely dimensional.

To overcome the limitations mentioned above, we suggest a state feedback scheme to accomplish the control of the Hopf bifurcation arising from system (1). We propose a nonlinear state feedback controller for the first equation of model (1) as follows:

$$\begin{aligned} u = &-\alpha_1(x(t) - x^*) - \alpha_2(x(t) - x^*)^2 \\ &-\alpha_3(x(t) - x^*)^3, \end{aligned} \tag{7}$$

where α_1, α_2, and α_3 are positive feedback gain parameters.

Remark 2 The controller (7) remains the equilibrium $E^*(x^*, p^*)$ of system (1) unchanged. Thus, the bifurcation control can be realized without destroying the properties of the original system (1).

Remark 3 The linear term $-\alpha_1(x(t) - x^*)$ is used only to relocate the onset of the Hopf bifurcation to a desired location, while the higher order terms $-\alpha_2(x(t) - x^*)^2 - \alpha_3(x(t) - x^*)^3$ can be used to regulate the properties of the Hopf bifurcation.

Remark 4 The nonlinear state feedback control (7) has the advantage of not requiring prior knowledge of anything but the natural x^* of system (1); so, it has been successfully used in quite diverse experimental contexts.

Remark 5 The state feedback scheme has been successfully used to control the Hopf bifurcation in various autonomous systems [3,6,10]. However, we first apply this scheme to a time-delayed system.

With the nonlinear state feedback controller (7), the controlled exponential RED algorithm model (1) becomes

$$\begin{aligned}\dot{x}(t) &= x(t-\tau)\left[\tfrac{1-p(t)}{\tau^2 x(t)} - kx(t)p(t)\right] \\ &\quad -\alpha_1(x(t)-x^*) - \alpha_2(x(t)-x^*)^2 \\ &\quad -\alpha_3(x(t)-x^*)^3, \\ \dot{p}(t) &= \tfrac{\beta}{c}p(t)(x(t-\tau)-c).\end{aligned} \tag{8}$$

3.1 Stability and existence of bifurcation for controlled system (8)

Let $u_1(t) = x(t) - x^*, u_2(t) = p(t) - p^*$. Then, (8) becomes

$$\begin{aligned}\dot{u}_1(t) &= (u_1(t-\tau)+c)\left[\tfrac{kc^2\tau^2-(1+kc^2\tau^2)u_2(t)}{\tau^2(1+kc^2\tau^2)(u_1(t)+c)}\right. \\ &\quad \left. -k(u_1(t)+c)(u_2(t)+\tfrac{1}{1+kc^2\tau^2})\right] \\ &\quad -\alpha_1 u_1(t) - \alpha_2 u_1^2(t) - \alpha_3 u_1^3(t), \\ \dot{u}_2(t) &= \tfrac{\beta}{c}\left(u_2(t)+\tfrac{1}{1+kc^2\tau^2}\right)u_1(t-\tau).\end{aligned} \tag{9}$$

Linearizing (9) about (0, 0) produces

$$\begin{aligned}\dot{u}_1(t) &= \left(-\tfrac{2kc}{1+kc^2\tau^2} - \alpha_1\right)u_1(t) - \tfrac{1+kc^2\tau^2}{\tau^2}u_2(t), \\ \dot{u}_2(t) &= \tfrac{\beta}{c(1+kc^2\tau^2)}u_1(t-\tau),\end{aligned} \tag{10}$$

which has the characteristic equation:

$$\lambda^2 + \left(\frac{2kc}{1+kc^2\tau^2} + \alpha_1\right)\lambda + \frac{\beta}{c\tau^2}e^{-\lambda\tau} = 0. \tag{11}$$

In what follows, we regard β as the bifurcation parameter to investigate the distribution of the roots to (11).

Lemma 1 *If $\alpha_1 > 0$, then there exists a minimum positive number β_0^c such that*

(i) *(11) has a pair of purely imaginary roots $\pm i\omega_0^c$ when $\beta = \beta_0^c$.*
(ii) *all the roots of (11) have negative real parts when $\beta \in (0, \beta_0^c)$.*
(iii) *$\beta_0^c > \beta_0$, where β_0 is defined by (3)–(5).*

Here,

$$\beta_0^c = c\tau^2\sqrt{(\omega_0^c)^4 + \left(\frac{2kc}{1+kc^2\tau^2}+\alpha_1\right)^2(\omega_0^c)^2}, \tag{12}$$

and

$$\omega_0^c \in \left(0, \frac{\pi}{2\tau}\right) \tag{13}$$

is the root of the equation

$$\frac{1}{\frac{2kc}{1+kc^2\tau^2}+\alpha_1}\omega = \cot(\omega\tau). \tag{14}$$

Proof (i) If $\lambda = i\omega$ ($\omega > 0$) is a pure imaginary solution of (11), it is straightforward to obtain that

$$\begin{aligned}\omega^2 &= \tfrac{\beta}{c\tau^2}\cos(\omega\tau), \\ \left(\tfrac{2kc}{1+kc^2\tau^2}+\alpha_1\right)\omega &= \tfrac{\beta}{c\tau^2}\sin(\omega\tau).\end{aligned} \tag{15}$$

Taking the ratio of the two equations of (15) yields (14). Solutions of (14) are the horizontal coordinates of the intersecting points between the curve $y = \cot(\omega\tau)$ and the line $y = \frac{1}{(\frac{2kc}{1+kc^2\tau^2}+\alpha_1)\tau}\omega\tau$. There are infinite numbers of intersecting points for these two curves that are graphically illustrated in Fig. 2.

Let ω_0^c satisfy (13) and be the root of (14) and define β_0^c as in (12). Then, (β_0^c, ω_0^c) is a solution of (15). Thus, $\pm i\omega_0^c$ is a pair of purely imaginary roots of (11) when $\beta = \beta_0^c$. It is easily seen form Fig. 2 that $\tau\omega_0^c$ is the minimum positive value among all horizontal coordinates of the intersecting points. So, β_0^c is the first value of $\beta > 0$ such that (11) has root appearing on the imaginary axis. The conclusion (i) follows.

(ii) When $\beta = 0$, the root of (11) is

$$\lambda_1 = -\left(\frac{2kc}{1+kc^2\tau^2}+\alpha_1\right) < 0, \quad \lambda_2 = 0.$$

Let $\lambda_2(\beta)$ be a root of (11) satisfying $\lambda_2(0) = 0$. We can obtain that

$$\lambda_2'(0) = -\frac{1}{\left(\frac{2kc}{1+kc^2\tau^2}+\alpha_1\right)c\tau^2} < 0.$$

Thus, all roots of (11) have negative real parts when $\beta \in (0, \beta_0^c)$. The conclusion (ii) follows.

(iii) It is clear from Fig. 2 that $\tau\omega_0$ is the horizontal coordinate of the intersecting point between the curve $y = \cot(\omega\tau)$ and the line $y = \frac{1}{\frac{2kc}{1+kc^2\tau^2}\tau}\omega\tau$, while $\tau\omega_0^c$ is the horizontal coordinate of the intersecting point between the curve $y = \cot(\omega\tau)$ and the line $y = \frac{1}{(\frac{2kc}{1+kc^2\tau^2}+\alpha_1)\tau}\omega\tau$.

If $\alpha_1 > 0$ holds, we have $\frac{1}{\frac{2kc}{1+kc^2\tau^2}\tau} > \frac{1}{(\frac{2kc}{1+kc^2\tau^2}+\alpha_1)\tau}$. Therefore, $\tau\omega_0^c > \tau\omega_0$, i.e., $\omega_0^c > \omega_0$. From the definitions of β_0 and β_0^c in (3) and (12), respectively, we can obtain that β_0^c is larger than β_0. The conclusion (iii) follows. Then the proof is completed. □

Remark 6 If the controller u is removed from the controlled system (8), i.e., $\alpha_1 = \alpha_2 = \alpha_3 = 0$, then (12) can be identical with the expression of β_0 in Theorem 1. Therefore, β_0 in Theorem 1 is a special case of β_0^c in (12) in the absence of the control.

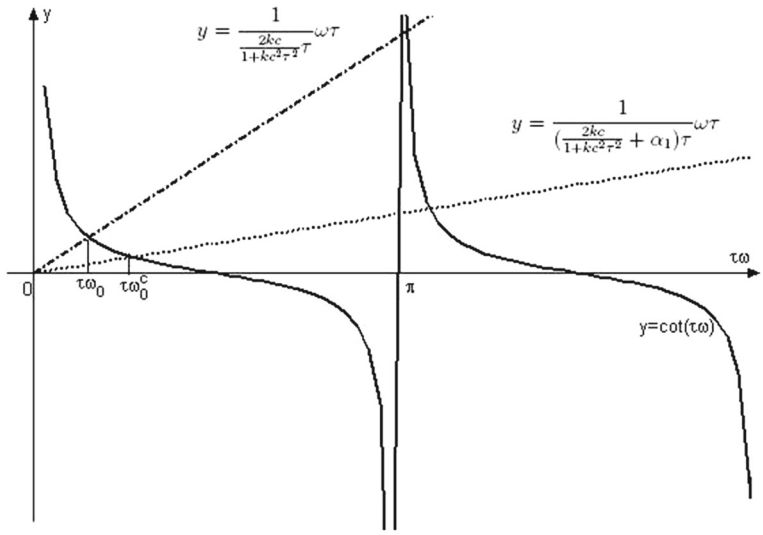

Fig. 2 The illustration for intersecting points between the curve $y = \cot(\omega\tau)$ and the line $y = \frac{1}{\frac{2kc}{1+kc^2\tau^2}\tau}\omega\tau$ or the curve $y = \frac{1}{(\frac{2kc}{1+kc^2\tau^2}+\alpha_1)\tau}\omega\tau$

In the following, we will show that the transversality condition of the Hopf bifurcation is also satisfied.

Lemma 2 *Let $\lambda(\beta) = \rho(\beta) + i\omega(\beta)$ be the root of (11) near $\beta = \beta_0^c$ satisfying $\rho(\beta_0^c) = 0, \omega(\beta_0^c) = \omega_0^c$. Suppose that $\alpha_1 > 0$ holds. Then,*

$$\frac{d}{d\beta}[Re\lambda]_{\beta=\beta_0^c} > 0.$$

Proof Differentiating (11) on β and applying the implicit function theorem, we have

$$\left[2\lambda+\left(\frac{2kc}{1+kc^2\tau^2}+\alpha_1\right)-\frac{\beta}{c\tau}e^{-\lambda\tau}\right]\frac{\mathrm{d}\lambda}{\mathrm{d}\beta}+\frac{1}{c\tau^2}e^{-\lambda\tau}=0,$$

and hence

$$\frac{\mathrm{d}\lambda}{\mathrm{d}\beta} = \frac{-\frac{1}{c\tau^2}e^{-\lambda\tau}}{2\lambda+\left(\frac{2kc}{1+kc^2\tau^2}+\alpha_1\right)-\frac{\beta}{c\tau}e^{-\lambda\tau}}.$$

Since $\lambda(\beta_0^c) = \mathrm{i}\omega_0^c$, it is obvious that

$$\begin{aligned}
&\left.\frac{\mathrm{d}\lambda}{\mathrm{d}\beta}\right|_{\beta=\beta_0^c}\\
&= \frac{-\frac{1}{c\tau^2}\cos(\omega_0^c\tau)+\mathrm{i}\frac{1}{c\tau^2}\sin(\omega_0^c\tau)}{\left[\left(\frac{2kc}{1+kc^2\tau^2}+\alpha_1\right)-\frac{\beta_0^c}{c\tau}\cos(\omega_0^c\tau)\right]+\mathrm{i}\left[2\omega_0^c+\frac{\beta_0^c}{c\tau}\sin(\omega_0^c\tau)\right]}\\
&= \frac{\frac{\left(\frac{2kc}{1+kc^2\tau^2}+\alpha_1\right)(\omega_0^c)^2}{\beta_0^c}+\frac{\beta_0^c}{c^2\tau^3}}{\left[\left(\frac{2kc}{1+kc^2\tau^2}+\alpha_1\right)-\frac{\beta_0^c}{c\tau}\cos(\omega_0^c\tau)\right]^2+\left[2\omega_0^c+\frac{\beta_0^c}{c\tau}\sin(\omega_0^c\tau)\right]^2}\\
&\quad+\mathrm{i}\frac{\frac{2(\omega_0^c)^3+\left(\frac{2kc}{1+kc^2\tau^2}+\alpha_1\right)^2\omega_0^c}{\beta_0^c}}{\left[\left(\frac{2kc}{1+kc^2\tau^2}+\alpha_1\right)-\frac{\beta_0^c}{c\tau}\cos(\omega_0^c\tau)\right]^2+\left[2\omega_0^c+\frac{\beta_0^c}{c\tau}\sin(\omega_0^c\tau)\right]^2}.
\end{aligned}$$

Thus, we can obtain

$$\begin{aligned}
&\frac{\mathrm{d}}{\mathrm{d}\beta}[Re\lambda]_{\beta=\beta_0^c}\\
&= \frac{\frac{\left(\frac{2kc}{1+kc^2\tau^2}+\alpha_1\right)(\omega_0^c)^2}{\beta_0^c}+\frac{\beta_0^c}{c^2\tau^3}}{\left[\left(\frac{2kc}{1+kc^2\tau^2}+\alpha_1\right)-\frac{\beta_0^c}{c\tau}\cos(\omega_0^c\tau)\right]^2+\left[2\omega_0^c+\frac{\beta_0^c}{c\tau}\sin(\omega_0^c\tau)\right]^2},
\end{aligned}\tag{16}$$

and

$$\begin{aligned}
&\frac{\mathrm{d}}{\mathrm{d}\beta}[\mathrm{Im}\lambda]_{\beta=\beta_0^c}\\
&= \frac{\frac{2(\omega_0^c)^3+\left(\frac{2kc}{1+kc^2\tau^2}+\alpha_1\right)^2\omega_0^c}{\beta_0^c}}{\left[\left(\frac{2kc}{1+kc^2\tau^2}+\alpha_1\right)-\frac{\beta_0^c}{c\tau}\cos(\omega_0^c\tau)\right]^2+\left[2\omega_0^c+\frac{\beta_0^c}{c\tau}\sin(\omega_0^c\tau)\right]^2}.
\end{aligned}$$

Since $\alpha_1 > 0$, it is clear that

$$\frac{\mathrm{d}}{\mathrm{d}\beta}[Re\lambda]_{\beta=\beta_0^c} > 0.$$

This completes the proof. □

From Lemma 2, we can obtain the following lemma.

Lemma 3 (14) *has at least one root with positive real part when $\beta > \beta_0^c$.*

From Lemmas 1–3 and the Hopf bifurcation theorems for functional differential equations (FDEs) in [32], we have the following results.

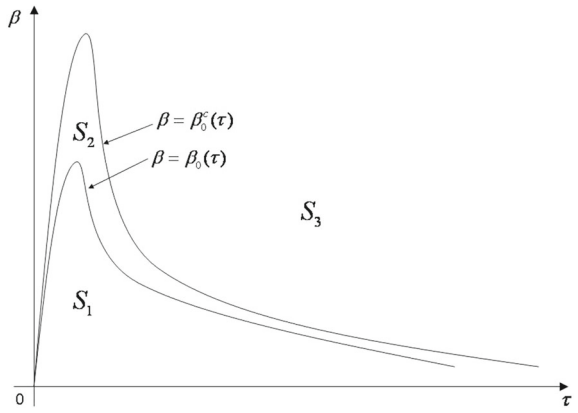

Fig. 3 The curves of β_0 and β_0^c depending on τ divide the first quadrant of (τ, β)-plane into three regions, S_1, S_2, and S_3. For the uncontrolled system (1), S_1 is a stable region, and $S_2 \cup S_3$ is an unstable region. For the controlled system (8), $S_1 \cup S_2$ is a stable region, and S_3 is an unstable region

Theorem 4 *Let $\alpha_1 > 0$, we have*

(i) *when $\beta \in (0, \beta_0^c)$, the non-zero equilibrium E^* of the controlled system (8) is locally asymptotically stable.*

(ii) *when $\beta > \beta_0^c$, the E^* of the controlled system (8) is unstable.*

(iii) *when $\beta = \beta_0^c$, the controlled system (8) exhibits a Hopf bifurcation at E^*, where $\beta_0^c > \beta_0$ is defined by (12)–(14), and the equilibrium E^* is kept unchanged.*

Remark 7 Theorem 4 indicates that under the control (7), one can delay or advance the onset of β_0 in Theorem 1 to β_0^c without changing the original equilibrium E^* by choosing an appropriate feedback gain parameter value of α_1. Thus, if one only needs to change the onset of the Hopf bifurcation, a linear state feedback control with the parameter α_1 is sufficient.

Remark 8 The stability domain of the original model (1) can be extended from S_1 to $S_1 \cup S_2$ under the state feedback control (7) (see Fig. 3). Therefore, one can guarantee a stationary sending rate for large parameter values, which benefits the decongestion.

3.2 Direction and stability of the Hopf bifurcation for controlled system (8)

Next, we will study the properties of the Hopf bifurcation of the controlled system (8) by the center manifold and normal form theories [33].

Applying Taylor expansion to the right-hand side of system (8) at the equilibrium, E^*, we have

$$\begin{aligned}\dot{u}_1(t) =& a_1u_1(t)+a_2u_2(t)+a_3u_1^2(t)+a_4u_1(t)u_2(t)\\ &+ a_5u_1(t-\tau)u_1(t)\\ &+ a_6u_1(t-\tau)u_2(t)+a_7u_1^3(t)+a_8u_1^2(t)u_2(t)\\ &+ a_9u_1(t-\tau)u_1^2(t)\\ &+ a_{10}u_1(t-\tau)u_1(t)u_2(t)+\text{h.o.t.},\\ \dot{u}_2(t) =& b_1u_1(t-\tau)+b_2u_1(t-\tau)u_2(t),\end{aligned} \tag{17}$$

where

$$\begin{aligned} a_1 &= -\left(\tfrac{2kc}{1+kc^2\tau^2}+\alpha_1\right), & a_2 &= -\tfrac{1+kc^2\tau^2}{\tau^2},\\ a_3 &= \tfrac{k}{1+kc^2\tau^2}-\alpha_2, & a_4 &= \tfrac{1-kc^2\tau^2}{c\tau^2},\\ a_5 &= -\tfrac{2k}{1+kc^2\tau^2}, & a_6 &= -\tfrac{1+kc^2\tau^2}{c\tau^2},\\ a_7 &= -\left[\tfrac{k}{c(1+kc^2\tau^2)}+\alpha_3\right], & a_8 &= -\tfrac{1}{c^2\tau^2},\\ a_9 &= \tfrac{k}{c(1+kc^2\tau^2)}, & a_{10} &= \tfrac{1-kc^2\tau^2}{c^2\tau^2},\\ b_1 &= \tfrac{\beta}{c(1+kc^2\tau^2)}, & b_2 &= \tfrac{\beta}{c}. \end{aligned}$$

For convenience, let $\beta = \beta_0^c + \mu$ and $u(t) = (u_1(t), u_2(t))^T$, where β_0^c is defined by (12)–(14) and $\mu \in R$; then system (17) can be written in a FDE in $C = C([-\tau, 0], R^2)$ as

$$\dot{u}(t) = L_\mu(u_t) + F(\mu, u_t), \tag{18}$$

where $u_t(\theta) = u(t+\theta) \in C$, and $L_\mu : C \to R^2$, $F : R \times C \to R^2$ are given, respectively, by

$$L_\mu(\phi) = B_1\phi(0) + B_2\phi(-\tau) \tag{19}$$

and

$$\begin{aligned}&F(\mu, \phi)\\ &= \begin{pmatrix} a_3\phi_1^2(0)+a_4\phi_1(0)\phi_2(0)+a_5\phi_1(-\tau)\phi_1(0)\\ \quad + a_6\phi_1(-\tau)\phi_2(0)+a_7\phi_1^3(0)+a_8\phi_1^2(0)\phi_2(0)\\ \quad + a_9\phi_1(-\tau)\phi_1^2(0)+a_{10}\phi_1(-\tau)\phi_1(0)\phi_2(0)+\text{h.o.t.}\\ b_2\phi_1(-\tau)\phi_2(0)\end{pmatrix},\end{aligned} \tag{20}$$

where $\phi(\theta) = (\phi_1(\theta), \phi_2(\theta))^T \in C$, and

$$B_1 = \begin{pmatrix} a_1 & a_2\\ 0 & 0\end{pmatrix}, \quad B_2 = \begin{pmatrix} 0 & 0\\ b_1 & 0\end{pmatrix}.$$

By the Riesz representation theorem, there exists a function $\eta(\theta, \mu)$ of bounded variation for $\theta \in [-\tau, 0]$, such that

$$L_\mu\phi = \int_{-\tau}^{0} \mathrm{d}\eta(\theta, \mu)\phi(\theta) \quad \text{for } \phi \in C,$$

which can be satisfied by choosing

$$\eta(\theta,\mu)=B_1\delta(\theta)-B_2\delta(\theta+\tau),$$

where δ is the Dirac delta function.

For $\phi\in C^1([-\tau,0],R^2)$, define

$$A(\mu)\phi=\begin{cases}\frac{\mathrm{d}\phi(\theta)}{\mathrm{d}\theta}, & \theta\in[-\tau,0),\\ \int_{-\tau}^{0}\mathrm{d}\eta(\mu,s)\phi(s), & \theta=0,\end{cases}$$

and

$$R(\mu)\phi=\begin{cases}0, & \theta\in[-\tau,0),\\ F(\mu,\phi), & \theta=0.\end{cases}$$

Then, system (18) is equivalent to

$$\dot{u}_t=A(\mu)u_t+R(\mu)u_t, \tag{21}$$

where $u_t(\theta)=u(t+\theta)$ for $\theta\in[-\tau,0]$.

For $\psi\in C([0,\tau],(R^2)^*)$, define

$$A^*\psi(s)=\begin{cases}-\frac{\mathrm{d}\psi(s)}{\mathrm{d}s}, & s\in(0,\tau],\\ \int_{-\tau}^{0}\mathrm{d}\eta^T(t,0)\psi(-t), & s=0,\end{cases}$$

and a bilinear inner product

$$\langle\psi(s),\phi(\theta)\rangle=\overline{\psi}(0)\phi(0)-\int_{\theta=-\tau}^{0}\int_{\xi=0}^{\theta}\overline{\psi}^T(\xi-\theta)\mathrm{d}\eta(\theta)\phi(\xi)\mathrm{d}\xi, \tag{22}$$

where $\eta(\theta)=\eta(\theta,0)$. Then, $A(0)$ and A^* are adjoint operators.

In order to determine the Poincare normal form of the operator $A(0)$, we need to calculate the eigenvector q of $A(0)$ corresponding to the eigenvalue $\mathrm{i}\omega_0^c$ and the eigenvector q^* of A^* corresponding to the eigenvalue $-\mathrm{i}\omega_0^c$. We can easily verify that

$$q(\theta)=(1,\gamma)^T\exp(\mathrm{i}\omega_0^c\theta),\quad \gamma=\frac{\mathrm{i}\omega_0^c-a_1}{a_2},$$

is the eigenvector of $A(0)$ corresponding to the eigenvalue $\mathrm{i}\omega_0^c$, and

$$q^*(s)=D(1,\gamma^*)^T\exp(\mathrm{i}\omega_0^c s),\quad \gamma^*=-\frac{a_2}{\mathrm{i}\omega_0^c},$$

is the eigenvector of A^* corresponding to $-\mathrm{i}\omega_0^c$.

By (22), we get

$$\begin{aligned}\langle q^*(s),q(\theta)\rangle&=\overline{D}\left\{1+\gamma\overline{\gamma^*}-\int_{-\tau}^{0}(1,\overline{\gamma^*})\theta e^{\mathrm{i}\theta\omega_0^c}\mathrm{d}\eta(\theta)(1,\gamma)^T\right\}\\&=\overline{D}\left(1+\gamma\overline{\gamma^*}+b_1\overline{\gamma^*}\tau e^{-\mathrm{i}\omega_0^c\tau}\right).\end{aligned}$$

Thus, we can choose

$$D=\left(1+\overline{\gamma}\gamma^*+b_1\gamma^*\tau e^{\mathrm{i}\omega_0^c\tau}\right)^{-1}$$

such that $\langle q^*(s),q(\theta)\rangle=1$.

In the following, we apply the ideas in Hassard et al. [33] to compute the coordinates describing the center manifold C_0 at $\mu=0$. Let u_t be the solution of (21) when $\mu=0$. We define

$$z(t)=\langle q^*,u_t\rangle,\ W(t,\theta)=u_t(\theta)-2Re\{z(t)q(\theta)\}. \tag{23}$$

On the center manifold C_0, we have

$$W(t,\theta)=W(z(t),\bar{z}(t),\theta),$$

where

$$W(z,\bar{z},\theta)=W_{20}(\theta)\frac{z^2}{2}+W_{11}(\theta)z\bar{z}+W_{02}(\theta)\frac{\bar{z}^2}{2}+W_{30}(\theta)\frac{z^3}{6}+\cdots, \tag{24}$$

z and $\bar{z}$ are local coordinates for center manifold C_0 in the direction of q^* and $\overline{q^*}$. Note that W is real if u_t is real. We only consider real solution. For the solution $u_t\in C_0$ of (21), since $\mu=0$, we have

$$\begin{aligned}\dot{z}(t)&=\langle q^*,\dot{u}_t\rangle\\&=\langle q^*,A(0)u_t\rangle+\langle q^*,R(0)u_t\rangle\\&=\langle A^*q^*,u_t\rangle+\overline{q^*}(0)F(0,u_t)\\&=\mathrm{i}\omega_0^c z(t)+\overline{q^*}(0)f_0(z,\bar{z}).\end{aligned}$$

We rewrite this equation as

$$\dot{z}(t)=\mathrm{i}\omega_0^c z(t)+g(z,\bar{z}), \tag{25}$$

with

$$g(z,\bar{z})=\overline{q^*}(0)f_0(z,\bar{z})=g_{20}\frac{z^2}{2}+g_{11}z\bar{z}+g_{02}\frac{\bar{z}^2}{2}+g_{21}\frac{z^2\bar{z}}{2}+\cdots. \tag{26}$$

By (23), we have $u_t(\theta)=(u_{1t}(\theta),u_{2t}(\theta))^T=W(t,\theta)+zq(\theta)+\bar{z}\bar{q}(\theta)$ and $q(\theta)=(1,\gamma)^T\exp(\mathrm{i}\omega_0^c\theta)$, and then

$$\begin{aligned}u_{1t}(0)&=z+\bar{z}+W_{20}^{(1)}(0)\frac{z^2}{2}+W_{11}^{(1)}(0)z\bar{z}+W_{02}^{(1)}(0)\frac{\bar{z}^2}{2}+O(|(z,\bar{z})|^3),\\u_{2t}(0)&=\gamma z+\overline{\gamma}\bar{z}+W_{20}^{(2)}(0)\frac{z^2}{2}+W_{11}^{(2)}(0)z\bar{z}+W_{02}^{(2)}(0)\frac{\bar{z}^2}{2}+O(|(z,\bar{z})|^3),\end{aligned}$$

$$u_{1t}(-\tau)=ze^{-i\omega_0^c\tau}+\bar{z}e^{i\omega_0^c\tau}+W_{20}^{(1)}(-\tau)\frac{z^2}{2}+W_{11}^{(1)}(-\tau)z\bar{z}+W_{02}^{(1)}(-\tau)\frac{\bar{z}^2}{2}+O(|(z,\bar{z})|^3),$$

$$u_{2t}(-\tau)=\gamma ze^{-i\omega_0^c\tau}+\overline{\gamma}\bar{z}e^{i\omega_0^c\tau}+W_{20}^{(2)}(-\tau)\frac{z^2}{2}+W_{11}^{(2)}(-\tau)z\bar{z}+W_{02}^{(2)}(-\tau)\frac{\bar{z}^2}{2}+O(|(z,\bar{z})|^3).$$

It follows together with (20) that

$$\begin{aligned}
g(z,\bar{z})&=\overline{q^*}(0)f_0(z,\bar{z})\\
&=\overline{D}\Big\{\Big[a_3+a_4\gamma+a_5e^{-i\omega_0^c\tau}+\left(a_6+b_2\overline{\gamma^*}\right)\gamma e^{-i\omega_0^c\tau}\Big]z^2\\
&+\Big[2a_3+a_4(\gamma+\overline{\gamma})+a_5\left(e^{i\omega_0^c\tau}+e^{-i\omega_0^c\tau}\right)+\left(a_6+b_2\overline{\gamma^*}\right)\left(\gamma e^{i\omega_0^c\tau}+\overline{\gamma}e^{-i\omega_0^c\tau}\right)\Big]z\bar{z}\\
&+\Big[a_3+a_4\overline{\gamma}+a_5e^{i\omega_0^c\tau}+\left(a_6+b_2\overline{\gamma^*}\right)\overline{\gamma}e^{i\omega_0^c\tau}\Big]\bar{z}^2\\
&+\Big[a_3\left(2W_{11}^{(1)}(0)+W_{20}^{(1)}(0)\right)+a_4\left(W_{11}^{(2)}(0)+\frac{1}{2}W_{20}^{(2)}(0)+\frac{1}{2}\overline{\gamma}W_{20}^{(1)}(0)+\gamma W_{11}^{(1)}(0)\right)\\
&+\left(a_6+b_2\overline{\gamma^*}\right)\left(\gamma W_{11}^{(1)}(-\tau)+\frac{1}{2}\overline{\gamma}W_{20}^{(1)}(-\tau)+\frac{1}{2}W_{20}^{(2)}(0)e^{i\omega_0^c\tau}+W_{11}^{(2)}(0)e^{-i\omega_0^c\tau}\right)+3a_7\\
&+a_8(\overline{\gamma}+2\gamma)+a_9\left(e^{i\omega_0^c\tau}+2e^{-i\omega_0^c\tau}\right)+a_{10}\left(\gamma e^{i\omega_0^c\tau}+\gamma e^{-i\omega_0^c\tau}+\overline{\gamma}e^{-i\omega_0^c\tau}\right)\\
&+a_5\left(W_{11}^{(1)}(-\tau)+\frac{1}{2}W_{20}^{(1)}(-\tau)+\frac{1}{2}W_{20}^{(1)}(0)e^{i\omega_0^c\tau}+W_{11}^{(1)}(0)e^{-i\omega_0^c\tau}\right)\Big]z^2\bar{z}+\cdots\Big\}.
\end{aligned}$$

Comparing the coefficients with (26), we have

$$\begin{aligned}
g_{20}&=2\overline{D}\Big[a_3+a_4\gamma+a_5e^{-i\omega_0^c\tau}+\left(a_6+b_2\overline{\gamma^*}\right)\gamma e^{-i\omega_0^c\tau}\Big];\\
g_{11}&=\overline{D}\Big[2a_3+a_4(\gamma+\overline{\gamma})+a_5\left(e^{i\omega_0^c\tau}+e^{-i\omega_0^c\tau}\right)+\left(a_6+b_2\overline{\gamma^*}\right)\left(\gamma e^{i\omega_0^c\tau}+\overline{\gamma}e^{-i\omega_0^c\tau}\right)\Big];\\
g_{02}&=2\overline{D}\Big[a_3+a_4\overline{\gamma}+a_5e^{i\omega_0^c\tau}+\left(a_6+b_2\overline{\gamma^*}\right)\overline{\gamma}e^{i\omega_0^c\tau}\Big];\\
g_{21}&=2\overline{D}\Big[a_3\left(2W_{11}^{(1)}(0)+W_{20}^{(1)}(0)\right)+a_4\left(W_{11}^{(2)}(0)+\frac{1}{2}W_{20}^{(2)}(0)+\frac{1}{2}\overline{\gamma}W_{20}^{(1)}(0)+\gamma W_{11}^{(1)}(0)\right)\\
&+\left(a_6+b_2\overline{\gamma^*}\right)\left(\gamma W_{11}^{(1)}(-\tau)+\frac{1}{2}\overline{\gamma}W_{20}^{(1)}(-\tau)+\frac{1}{2}W_{20}^{(2)}(0)e^{i\omega_0^c\tau}+W_{11}^{(2)}(0)e^{-i\omega_0^c\tau}\right)+3a_7\\
&+a_8(\overline{\gamma}+2\gamma)+a_9\left(e^{i\omega_0^c\tau}+2e^{-i\omega_0^c\tau}\right)+a_{10}\left(\gamma e^{i\omega_0^c\tau}+\gamma e^{-i\omega_0^c\tau}+\overline{\gamma}e^{-i\omega_0^c\tau}\right)\\
&+a_5\left(W_{11}^{(1)}(-\tau)+\frac{1}{2}W_{20}^{(1)}(-\tau)+\frac{1}{2}W_{20}^{(1)}(0)e^{i\omega_0^c\tau}+W_{11}^{(1)}(0)e^{-i\omega_0^c\tau}\right)\Big].
\end{aligned}\tag{27}$$

In order to determine g_{21}, in the sequel, we need to compute $W_{20}(\theta)$ and $W_{11}(\theta)$. From (21) and (23), we have

$$\begin{aligned}
\dot{W}&=\dot{u}_t-\dot{z}q-\dot{\bar{z}}\bar{q}\\
&=\begin{cases}A(0)W-2Re\{\overline{q^*}(0)f_0(z,\bar{z})q(\theta)\},&\theta\in[-\tau,0),\\A(0)W-2Re\{\overline{q^*}(0)f_0(z,\bar{z})q(0)\}+f_0(z,\bar{z}),&\theta=0,\end{cases}\\
&=A(0)W+H(z,\bar{z},\theta),
\end{aligned}\tag{28}$$

where

$$H(z,\bar{z},\theta)=H_{20}(\theta)\frac{z^2}{2}+H_{11}(\theta)z\bar{z}+H_{02}(\theta)\frac{\bar{z}^2}{2}+\cdots.\tag{29}$$

On the other hand, note that on the center manifold C_0 near to the origin,

$$\dot{W}=W_z\dot{z}+W_{\bar{z}}\dot{\bar{z}}.$$

This, together with (28) and (29), reads to

$$\begin{aligned}
&(A(0)-2i\omega_0^c)W_{20}(\theta)=-H_{20}(\theta),\\
&A(0)W_{11}(\theta)=-H_{11}(\theta),\\
&(A(0)+2i\omega_0^c)W_{02}(\theta)=-H_{02}(\theta),\ldots.
\end{aligned}\tag{30}$$

By (28), we know that for $\theta\in[-\tau,0)$,

$$\begin{aligned}
H(z,\bar{z},\theta)&=-\overline{q^*}(0)f_0(z,\bar{z})q(\theta)-q^*(0)\overline{f_0}(z,\bar{z})\overline{q}(\theta)\\
&=-g(z,\bar{z})q(\theta)-\overline{g}(z,\bar{z})\overline{q}(\theta)\\
&=-\left(g_{20}\tfrac{z^2}{2}+g_{11}z\bar{z}+g_{02}\tfrac{\bar{z}^2}{2}+\cdots.\right)q(\theta)\\
&\quad-\left(\overline{g}_{20}\tfrac{\bar{z}^2}{2}+\overline{g}_{11}z\bar{z}+\overline{g}_{02}\tfrac{z^2}{2}+\cdots.\right)\overline{q}(\theta).
\end{aligned}\tag{31}$$

Comparing the coefficients with (29) gives that

$$\begin{aligned}
H_{20}(\theta)&=-g_{20}q(\theta)-\overline{g}_{02}\overline{q}(\theta),\\
H_{11}(\theta)&=-g_{11}q(\theta)-\overline{g}_{11}\overline{q}(\theta).
\end{aligned}$$

It follows from (30) that

$$\begin{aligned}\dot{W}_{20}(\theta) &= 2\mathrm{i}\omega_0^c + g_{20}q(\theta) + \overline{g}_{02}\overline{q}(\theta),\\ \dot{W}_{11}(\theta) &= g_{11}q(\theta) + \overline{g}_{11}\overline{q}(\theta).\end{aligned} \tag{32}$$

Noticing that $q(\theta) = (1, \gamma)^T \exp(\mathrm{i}\omega_0^c\theta)$, we have

$$\begin{aligned}W_{20}(\theta) &= \frac{\mathrm{i}g_{20}}{\omega_0^c}q(0)e^{\mathrm{i}\omega_0^c\theta} + \frac{\mathrm{i}\overline{g}_{02}}{3\omega_0^c}\overline{q}(0)e^{-\mathrm{i}\omega_0^c\theta} + E_1 e^{2\mathrm{i}\omega_0^c\theta},\\ W_{11}(\theta) &= -\frac{\mathrm{i}g_{11}}{\omega_0^c}q(0)e^{\mathrm{i}\omega_0^c\theta} + \frac{\mathrm{i}\overline{g}_{11}}{\omega_0^c}\overline{q}(0)e^{-\mathrm{i}\omega_0^c\theta} + E_2,\end{aligned} \tag{33}$$

where E_1 and E_2 are constant vectors.

In what follows, we shall seek appropriate E_1 and E_2. From

$$H(z, \bar{z}, 0) = -2Re\left\{\overline{q^*}(0) f_0(z, \bar{z})q(0)\right\} + f_0(z, \bar{z}),$$

we obtain

$$H_{20}(0) = -g_{20}q(0) - \overline{g}_{02}\overline{q}(0) + A_1 \tag{34}$$

and

$$H_{11}(0) = -g_{11}q(0) - \overline{g}_{11}\overline{q}(0) + A_2, \tag{35}$$

where

$$A_1 = 2\begin{pmatrix} a_3 + a_4\gamma + a_5 e^{-\mathrm{i}\omega_0^c\tau} + a_6\gamma e^{-\mathrm{i}\omega_0^c\tau} \\ b_2\gamma e^{-\mathrm{i}\omega_0^c\tau}\end{pmatrix},$$

$$A_2 = 2\begin{pmatrix} 2a_3 + a_4(\gamma + \overline{\gamma}) + a_5\left(e^{\mathrm{i}\omega_0^c\tau} + e^{-\mathrm{i}\omega_0^c\tau}\right) \\ + a_6\left(\gamma e^{\mathrm{i}\omega_0^c\tau} + \overline{\gamma}e^{-\mathrm{i}\omega_0^c\tau}\right) \\ b_2\left(\gamma e^{\mathrm{i}\omega_0^c\tau} + \overline{\gamma}e^{-\mathrm{i}\omega_0^c\tau}\right)\end{pmatrix}.$$

From (30) and the definition of $A(0)$, we have

$$\begin{aligned}B_1W_{20}(0) + B_2W_{20}(-\tau) &= 2\mathrm{i}\omega_0^c W_{20}(0) - H_{20}(0),\\ B_1W_{11}(0) + B_2W_{11}(-\tau) &= -H_{11}(0).\end{aligned} \tag{36}$$

Substituting (33)–(35) into (36) and noticing that

$$\left(\mathrm{i}\omega_0^c I - \int_{-\tau}^{0} e^{\mathrm{i}\theta\omega_0^c}\mathrm{d}\eta(\theta)\right)q(0) = 0$$

and

$$\left(-\mathrm{i}\omega_0^c I - \int_{-\tau}^{0} e^{-\mathrm{i}\theta\omega_0^c}\mathrm{d}\eta(\theta)\right)\overline{q}(0) = 0,$$

we can obtain

$$\begin{aligned}E_1 &= \left(2\mathrm{i}\omega_0^c I - B_1 - B_2 e^{-2\mathrm{i}\omega_0^c\tau}\right)^{-1} A_1,\\ E_2 &= -\left(B_1 + B_2\right)^{-1} A_2.\end{aligned}$$

Therefore, each g_{ij} in (27) has been expressed in terms of the parameters and the delay given in system (8). Furthermore, we can compute the following quantities:

$$\begin{aligned}c_1(0) &= \frac{\mathrm{i}}{2\omega_0^c}\left(g_{11}g_{20} - 2|g_{11}|^2 - \frac{|g_{02}|^2}{3}\right) + \frac{g_{21}}{2},\\ \mu_2^c &= -\frac{Re\{c_1(0)\}}{Re\{\lambda'(\beta_0^c)\}},\\ \nu_2^c &= 2Re\{c_1(0)\},\\ T_2^c &= -\frac{\mathrm{Im}\{c_1(0)\} + \mu_2\mathrm{Im}\{\lambda'(\beta_0^c)\}}{\omega_0^c}.\end{aligned} \tag{37}$$

Now, the main results of this section are summarized as follows.

Theorem 5 *The Hopf bifurcation exhibited by the controlled exponential RED algorithm model (8) is determined by the parameters μ_2^c, ν_2^c, T_2^c, where μ_2^c determines the direction of the Hopf bifurcation: if $\mu_2^c > 0$ ($\mu_2^c < 0$), then the Hopf bifurcation is supercritical (subcritical) and the bifurcating periodic solutions exist for $\beta > \beta_0^c$ ($\beta < \beta_0^c$); ν_2^c determines the stability of the bifurcating periodic solutions: the bifurcating periodic solutions are stable (unstable) if $\nu_2^c < 0$ ($\nu_2^c > 0$); and T_2^c determines the period of the bifurcating periodic solutions: the period increases (decreases) if $T_2^c > 0$ ($T_2^c < 0$).*

Remark 9 Theorem 5 shows that one may choose appropriate values of the parameters α_1, α_2, and α_3 to change the values of μ_2, ν_2, T_2 in Theorems 3 in order to control the properties of the Hopf bifurcation of system (1).

4 Numerical simulations

To verify the effectiveness of the proposed control scheme, numerical results are employed in this section.

For a consistent comparison, the same model (1), used in [28], is discussed, with $c = 1, k = 0.8$, and $\tau = 5$. From (2), the uncontrolled system (1) has a unique non-zero equilibrium $E^* = (1, 0.0476)$. It follows from Theorems 1–3 that

$$\begin{aligned}&\beta_0 = 0.4032, \quad \omega_0 = 0.1161,\\ &\mu_2 = 0.0093, \quad \nu_2 = -0.0014, \quad T_2 = 1.9004.\end{aligned}$$

It is shown from Theorems 1 and 2 that when $\beta < \beta_0$, the equilibrium E^* is stable (see Fig. 4), while as β is increased to pass through β_0, E^* loses its

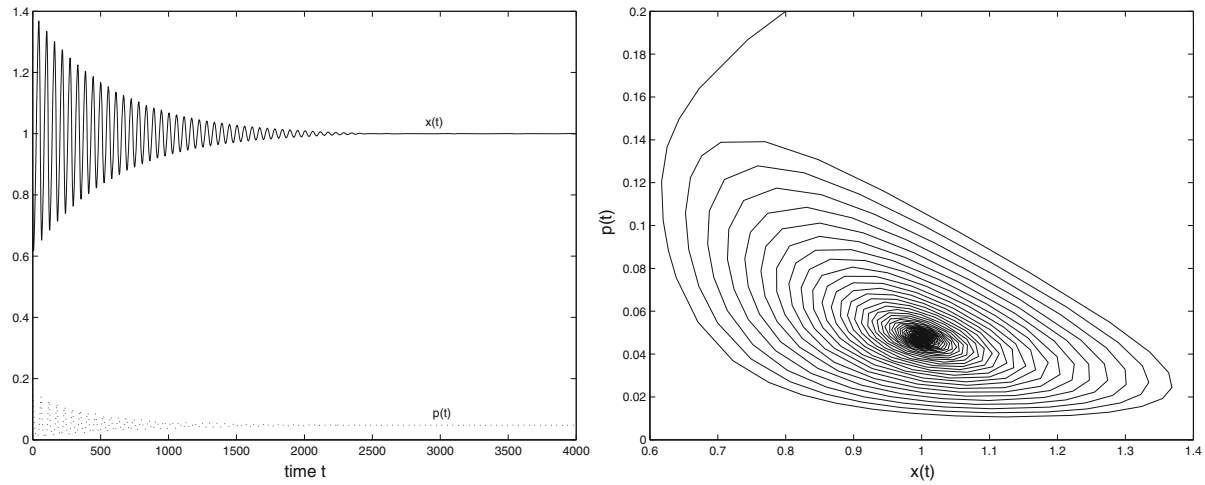

Fig. 4 Waveform plot and phase portrait of the uncontrolled model (1) with $c = 1, k = 0.8$, and $\tau = 5$. The equilibrium E^* is asymptotically stable, where $\beta = 0.38 < \beta_0 = 0.4032$

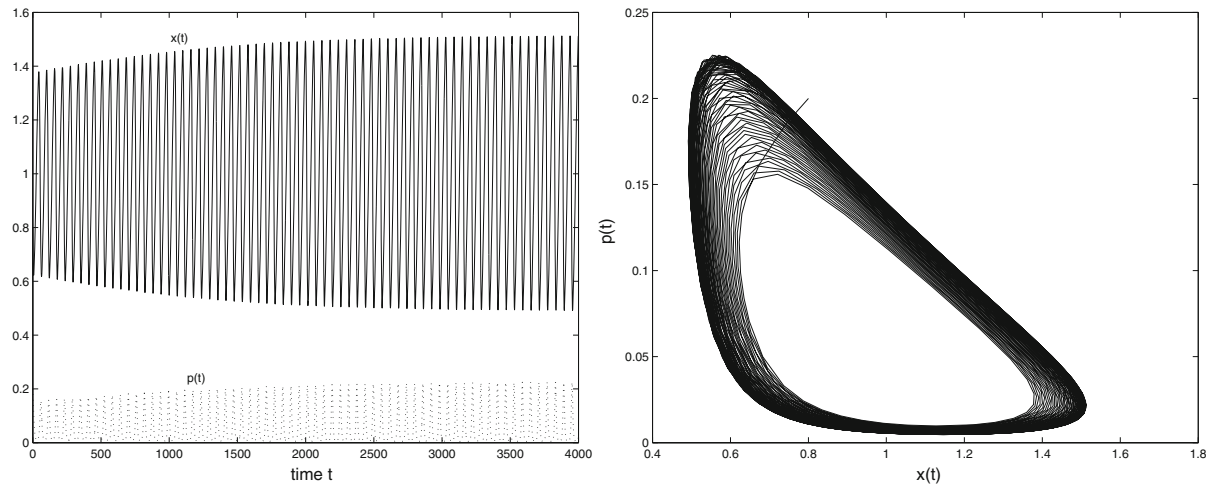

Fig. 5 Waveform plot and phase portrait of the uncontrolled model (1) with $c = 1, k = 0.8$, and $\tau = 5$. A periodic oscillation bifurcates from the equilibrium E^*, where $\beta = 0.408 > \beta_0 = 0.4032$

stability and a Hopf bifurcation occurs (see Figs. 5 and 6). Note that the periodic orbits are stable since $\nu_2 < 0$, the bifurcating periodic solutions exist at least for the value β slightly larger than the critical value β_0 since $\mu_2 > 0$, and the period of the periodic solutions increases as β increases due to $T_2 > 0$.

Next, we control the Hopf bifurcation based on the state feedback scheme.

Case 1 linear state feedback control.

It can be seen from Theorem 4 that for the linear state feedback control with an appropriate value of α_1, we can delay the onset of the Hopf bifurcation. For example, by choosing

$$\alpha_1 = 0.02, \quad \alpha_2 = 0, \quad \alpha_3 = 0,$$

we can apply Theorems 4 and 5 in Sect. 3 to obtain

$$\beta_0^c = 0.5157, \quad \omega_0^c = 0.1285,$$
$$\mu_2^c = 0.9964, \quad \nu_2^c = -0.5918, \quad T_2^c = 0.9322.$$

Note that the controlled model (8) has the same equilibrium point as that of the original model (1), but the critical value β_0 increases from 0.4032 to 0.5157, implying that the onset of the Hopf bifurcation is delayed.

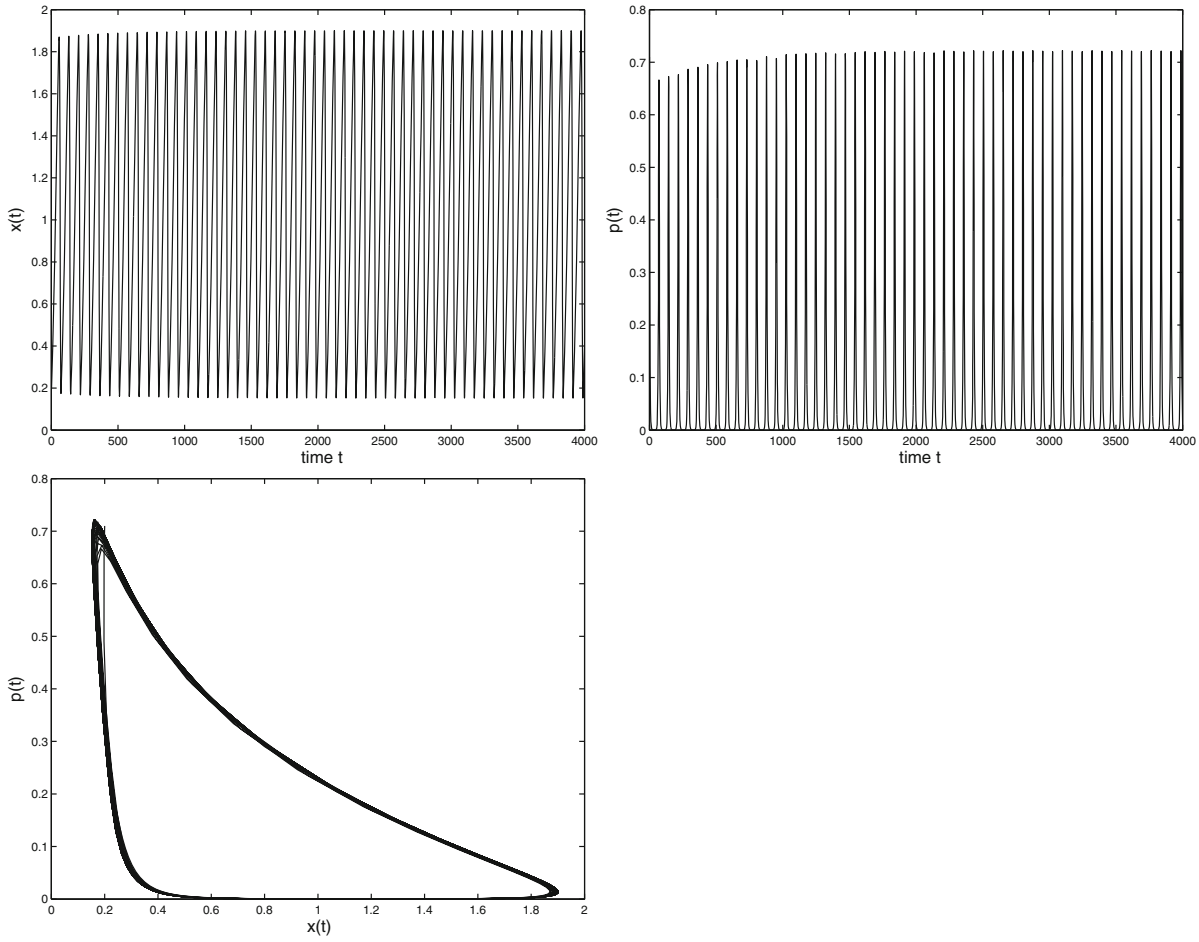

Fig. 6 Waveform plot and phase portrait of the uncontrolled model (1) with $c = 1$, $k = 0.8$, and $\tau = 5$. A periodic oscillation bifurcates from the equilibrium E^*, where $\beta = 0.435 > \beta_0 = 0.4032$

Under the linear state feedback control with $\alpha_1 = 0.02, \alpha_2 = \alpha_3 = 0$, we choose $\beta = 0.435 < \beta_0^c$, which is the same value as that used in Fig. 6. It can be concluded from Theorem 4 that instead of having a Hopf bifurcation, the equilibrium E^* of the controlled model (8) is stable, as shown in Fig. 7. However, the equilibrium E^* becomes unstable when $\beta = 0.54 > \beta_0^c$, as shown in Fig. 8. Moreover, when $\beta = 0.6 > \beta_0^c$, the equilibrium point E^* is also unstable, as shown in Fig. 9.

It is shown that when β passes the critical value $\beta_0^c = 0.5157$, a Hopf bifurcation occurs (see Figs. 8 and 9). The periodic orbits are stable since $\nu_2^c < 0$. Since $\mu_2^c > 0$, the bifurcating periodic solutions exist at least for the value β slightly larger than the critical value β_0^c. Since $T_2^c > 0$, the period of the periodic solutions increases as β increases.

If we choose a larger value of α_1, the exponential RED algorithm model may not have a Hopf bifurcation even for larger values of β. For example, when choosing $\alpha_1 = 0.3, \alpha_2 = \alpha_3 = 0$, the equilibrium E^* of the controlled model (8) is stable if $\beta < \beta_0^c = 2.2846$, as shown in Fig. 10. This indicates that the linear state feedback control can delay the onset of the Hopf bifurcation.

Figure 11 shows a local bifurcation diagram in terms of the parameter β for model (1) without and with the linear state feedback control. Solid and dashed curves denote the stable and unstable solutions, respectively.

Figure 12 displays the dependence of β_0^c upon the feedback gain α_1 according to the controlled system (8) for $c = 1, k = 0.8$, and $\alpha_2 = \alpha_2 = 0$. The dash-dotted curve corresponds to a delay of $\tau = 5$, the dotted curve to $\tau = 4.5$, the solid curve to $\tau = 4$, and

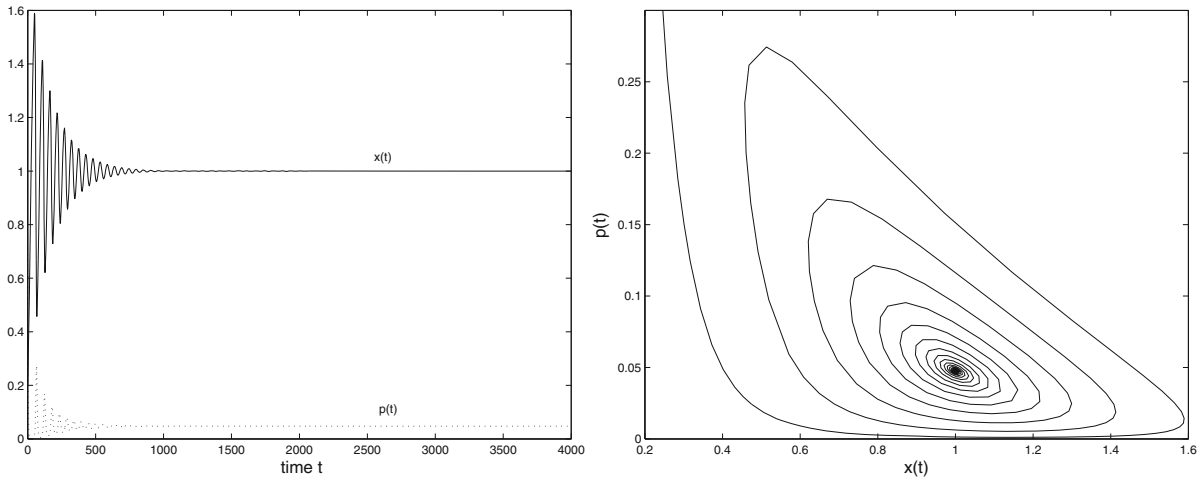

Fig. 7 Waveform plot and phase portrait of the controlled model (8) with $c = 1, k = 0.8, \tau = 5$, and $\alpha_1 = 0.02, \alpha_2 = \alpha_3 = 0$. The equilibrium E^* is asymptotically stable, where $0.4032 = \beta_0 < \beta = 0.435 < \beta_0^c = 0.5157$

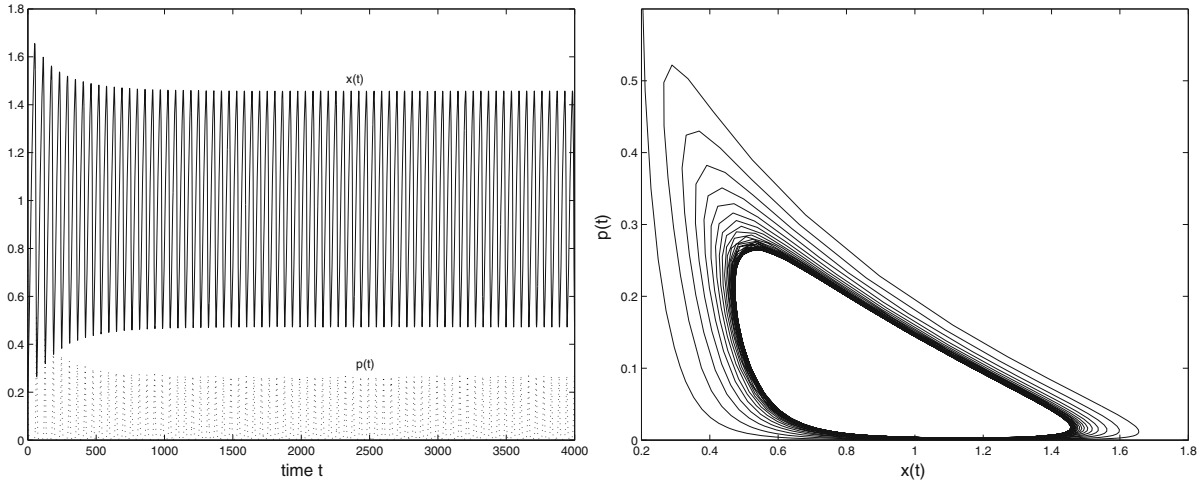

Fig. 8 Waveform plot and phase portrait of the controlled model (8) with $c = 1, k = 0.8, \tau = 5$, and $\alpha_1 = 0.02, \alpha_2 = \alpha_3 = 0$. A periodic oscillation bifurcates from the equilibrium E^*, where $\beta = 0.54 > \beta_0^c = 0.5157$

the dashed curve to $\tau = 3.5$. The values of the β_0^c are calculated by solving (12)–(14) numerically. For increasing the feedback gain α_1, the critical value β_0^c increases for a fixed time delay τ. Increasing α_1 postpones the onset of the Hopf bifurcation and reduces the instability. Hence, the control is successful. It also can be seen from Fig. 12 that when $\alpha_1 > 0.1$, increasing time delay of τ raises the value of β_0^c to a fixed feedback gain α_1; when $\alpha_1 < 0.1$, decreasing time delay of τ raises the value of β_0^c to a fixed feedback gain α_1.

Case 2 nonlinear state feedback control.

Different from the linear state feedback control discussed in Case 1, the nonlinear state feedback control has two more feedback gain parameters α_2 and α_3, which expands the regulated parameters besides the parameter α_1.

Although it may be enough to use only α_1 for model (1) in delaying the onset of the Hopf bifurcation, it is more effective to use all the three parameters in changing the properties of the Hopf bifurcation for the exponential RED algorithm model. Note that, under these

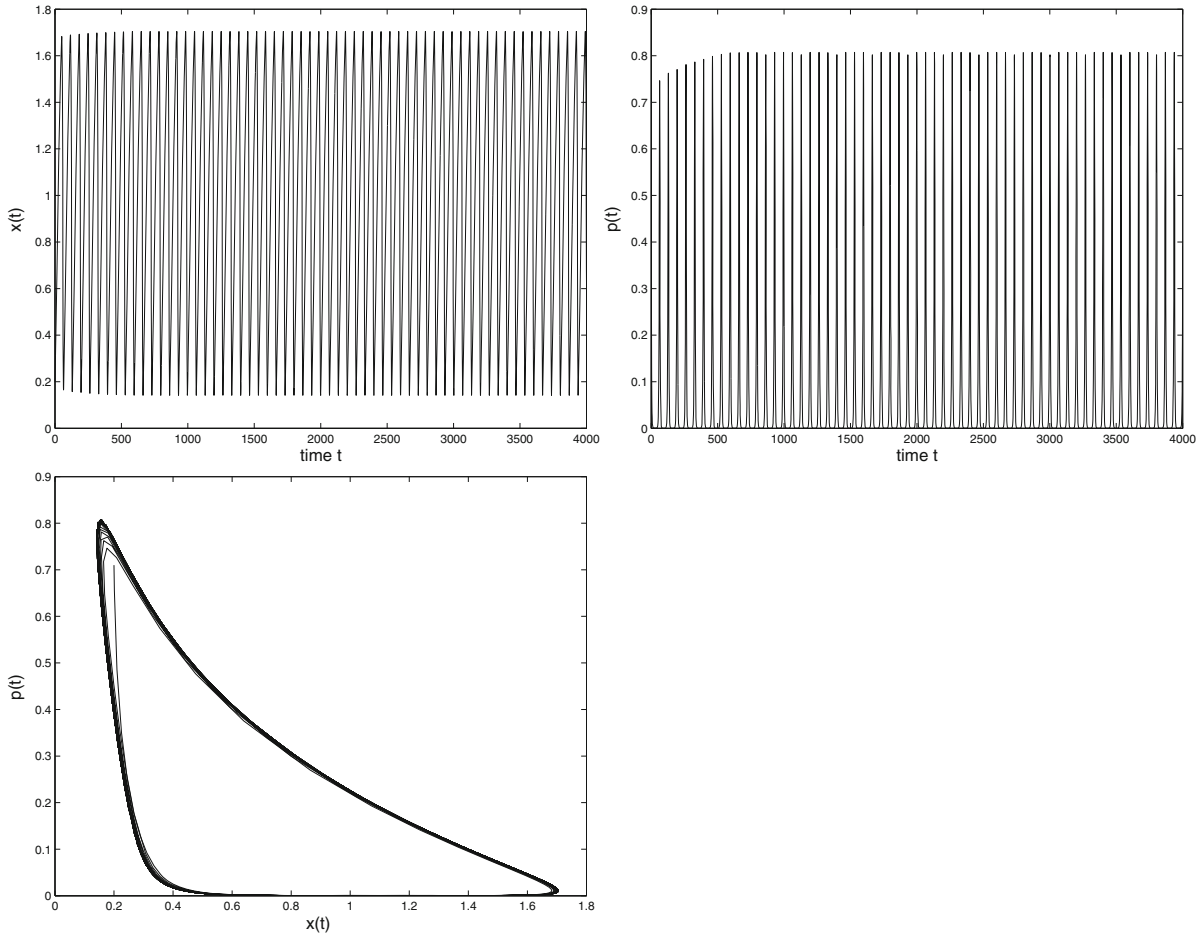

Fig. 9 Waveform plot and phase portrait of the controlled model (8) with $c = 1, k = 0.8, \tau = 5$, and $\alpha_1 = 0.02, \alpha_2 = \alpha_3 = 0$. A periodic oscillation bifurcates from the equilibrium E^*, where $\beta = 0.6 > \beta_0^c = 0.5157$

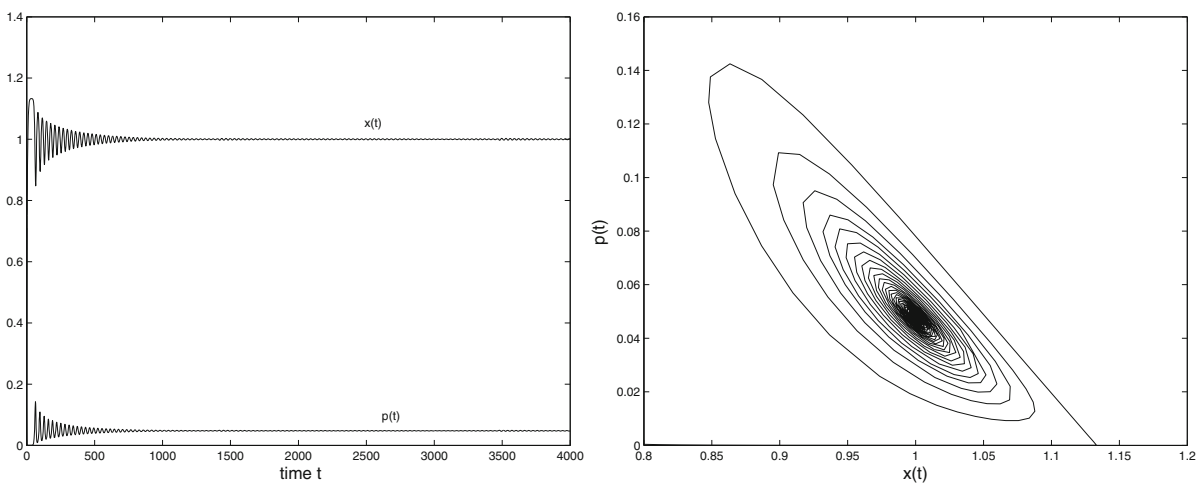

Fig. 10 Waveform plot and phase portrait of the controlled model (8) with $c = 1, k = 0.8, \tau = 5$, and $\alpha_1 = 0.3, \alpha_2 = \alpha_3 = 0$. The equilibrium E^* is asymptotically stable, where $\beta = 2.2 < \beta_0^c = 2.2846$

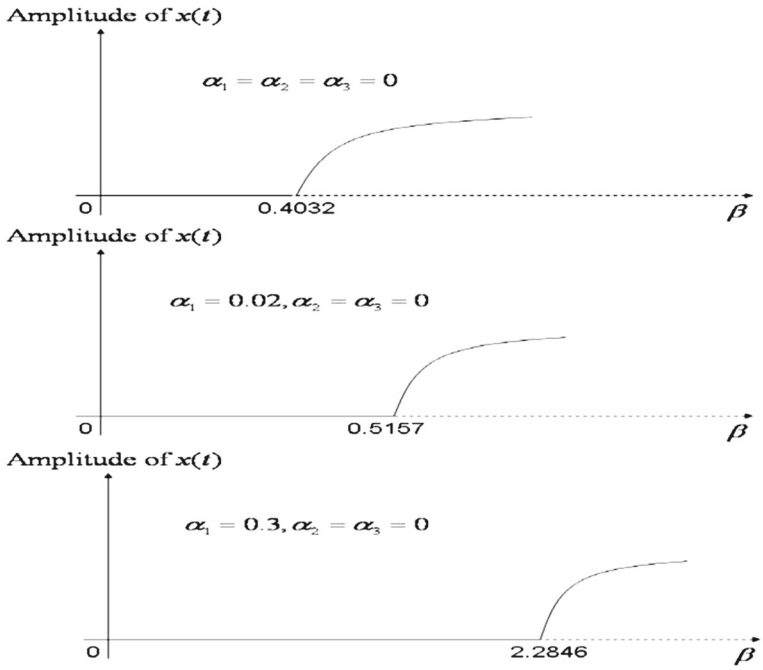

Fig. 11 Local bifurcation diagram of model (1) without and with the linear state feedback control

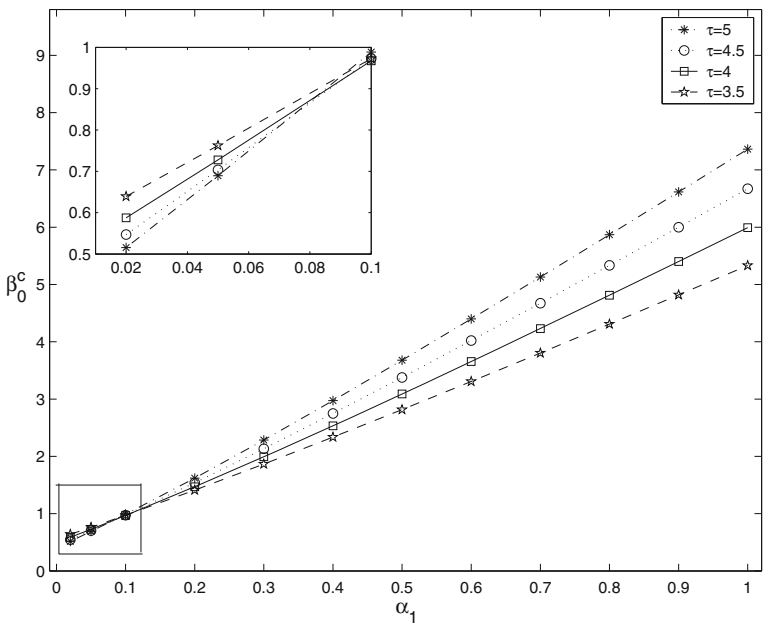

Fig. 12 The fluctuation of β_0^c depending on α_1 for $c = 1, k = 0.8$, and $\alpha_2 = \alpha_3 = 0$ as given by the controlled system (8)

three parameters, only parameters a_3 and a_7 are different from the linear state feedback control discussed in Case 1. The derivation of the formulas for this general nonlinear case can follow the same procedure described in Sect. 3. Choosing different values of α_1, α_2, and α_3, one can efficiently change the stability, direction, and period of the Hopf bifurcation. For example, when

$$\alpha_1 = 0.02, \quad \alpha_2 = 0.01, \quad \alpha_3 = 0.02,$$

we have

$$\mu_2^c = 0.1437, \quad \nu_2^c = -1.0587, \quad T_2^c = 0.0156.$$

The critical value $\beta_0^c = 0.5157$, and the equilibrium is the same as that in the Case 1 with $\alpha_1 = 0.02, \alpha_2 = \alpha_3 = 0$. Taking $\beta = 0.54$ yields the results shown in

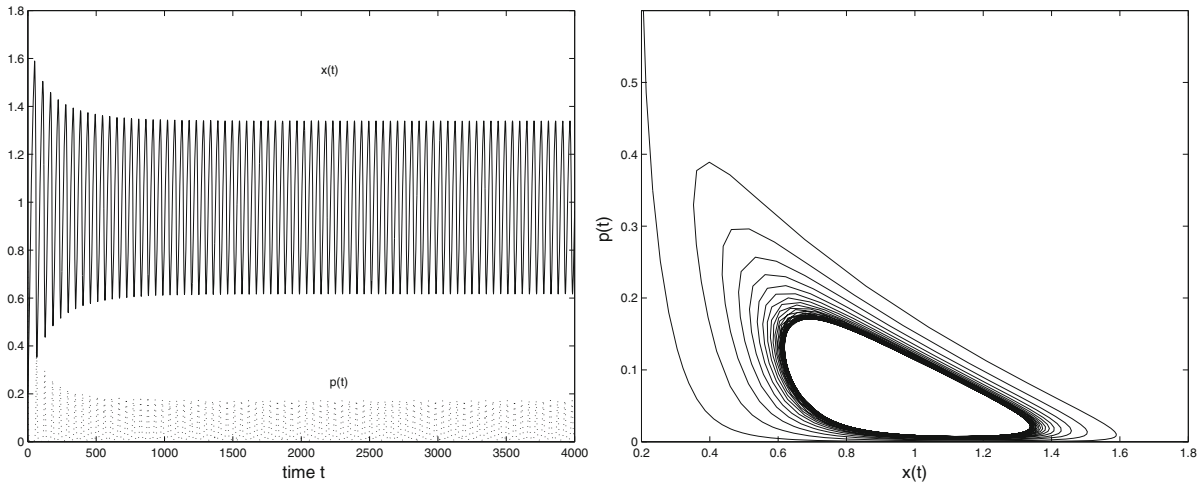

Fig. 13 Waveform plot and phase portrait of controlled model (8) with $\beta = 0.54$ and $\alpha_1 = 0.02, \alpha_2 = 0.01, \alpha_3 = 0.02$

Fig. 13, where β takes the same value as that of the case shown in Fig. 8. It is noted that the behavior shown in Fig. 13 is quite different from that of Fig. 8 even if a same value of β is used in the two cases. The amplitude of the limit cycle shown in Fig. 8 is larger than that depicted in Fig. 13. This can be explained by means of the approximate Hopf bifurcation solutions [34] that the absolute value of ν_2 given for Fig. 8 ($\nu_2 = -0.5918$) is smaller than that for Fig. 13 ($\nu_2 = -1.0587$), but the linear coefficient $Re'\lambda(\beta_0^c)$ is same for the two cases. This suggests that one may choose appropriate values of α_2 and α_3, in addition to α_1, to obtain the desired behavior of a Hopf bifurcation.

5 Conclusion

In this paper, a new control scheme is proposed based on the dynamic state feedback to control the Hopf bifurcation arising from a time-delayed exponential RED algorithm model. The conditions for the stability and bifurcation are obtained for the controlled exponential RED algorithm model by analyzing the characteristic equation. In addition, using the normal form theory and center manifold reduction, the direction of the Hopf bifurcation is determined. Numerical simulations are presented to verify the analytical results. It is shown that the linear state feedback control may be used to change the onset of the Hopf bifurcation, while the nonlinear state feedback control can be applied to regulate the properties of the Hopf bifurcation.

The future research is to apply this dynamic state feedback scheme to high-dimensional Internet congestion control systems.

Acknowledgments This work was supported in part by the National Natural Science Foundation of China (Grant Nos. 61203232, 61374180, and 71171050), the Natural Science Foundation of Jiangsu Province of China (Grant No. BK2012072), and the China Postdoctoral Science Foundation funded project (Grant No. 2013M530229).

References

1. Chen, G.R., Moiola, J.L., Wang, H.O.: Bifurcation control: theories, methods and applications. Int. J. Bifurc. Chaos **10**, 511–548 (2000)
2. Abed, E.H., Fu, J.H.: Local feedback stabilization and bifurcation control: I. Hopf bifurcation. Syst. Control Lett. **7**, 11–17 (1986)
3. Wang, H., Abed, E.H.: Bifurcation control of a chaotic system. Automatica **31**, 1213–1226 (1995)
4. Tesi, A., Abed, E.H., Genesio, R., Wang, H.O.: Harmonic balance analysis of period-doubling bifurcations with implications for control of nonlinear dynamics. Automatica **32**, 1255–1271 (1996)
5. Pyragas, K., Pyragas, V., Benner, H.: Delayed feedback control of dynamical systems at a subcritical Hopf bifurcation. Phys. Rev. E **70**, 056222 (2004)
6. Yu, P., Chen, G.R.: Hopf bifurcation control using nonlinear feedback with polynomial functions. Int. J. Bifurc. Chaos **14**, 1683–1704 (2004)
7. Just, W., Fiedler, B., Georgi, M., Flunkert, V., Hövel, P., Schöll, E.: Beyond the odd number limitation: a bifurcation analysis of time-delayed feedback control. Phys. Rev. E **76**, 026210 (2007)

8. Liu, F., Guan, Z., Wang, H., Li, Y.: Impulsive control of bifurcations. Math. Comput. Simul. **79**, 2180–2191 (2009)
9. Xiao, M., Daniel, W.C., Cao, J.: Time-delayed feedback control of dynamical small-world networks at Hopf bifurcation. Nonlinear Dyn. **58**, 319–344 (2009)
10. Nguyen, L.H., Hong, K.S.: Hopf bifurcation control via a dynamic state-feedback control. Phys. Lett. A **376**, 442–446 (2012)
11. Kelly, F.P., Maulloo, A.K., Tan, D.K.H.: Rate control for communication networks: shadow prices, proportional fairness and stability. J. Oper. Res. Soc. **49**, 237–252 (1998)
12. Jacobson, V.: Congestion avoidance and control. ACM SIGCOMM Comput. Commun. Rev. **18**, 314–329 (1998)
13. Huang, Z., Yang, Q., Cao, J.: The stochastic stability and bifurcation behavior of an Internet congestion control model. Math. Comput. Model. **54**, 1954–1965 (2011)
14. Floyd, S., Jacobson, V.: Random early detection gateways for congestion avoidance. IEEE Trans. Netw. **1**, 397–413 (1993)
15. Athuraliya, S., Low, S., Li, V., Yin, Q.: REM: active queue management. IEEE Trans. Netw. **15**, 48–53 (2001)
16. Gibbens, R., Kelly, F.: Resource pricing and the evolution of congestion control. Automatica **35**, 1969–1985 (1999)
17. Kunniyur, S., Srikant, R.: Analysis and design of adaptive virtual queue algorithm for active queue management. ACM Comput. Commun. Rev. **31**, 123–134 (2001)
18. Li, C.G., Chen, G.R., Liao, X.F.: Hopf bifurcation in an Internet congestion control model. Chaos Solitions Fractals **19**, 853–862 (2004)
19. Chen, Z., Yu, P.: Hopf bifurcation control for an Internet congestion model. Int. J. Bifurc. Chaos **15**, 2643–2651 (2005)
20. Xiao, M., Cao, J.: Delayed feedback-based bifurcation control in an Internet congestion model. J. Math. Anal. Appl. **332**, 1010–1027 (2007)
21. Xiao, M., Zheng, W.X., Cao, J.: Bifurcation control of a congestion control model via state feedback. Int. J. Bifurc. Chaos **23**, 1330018 (2013)
22. Ding, D., Zhu, J., Luo, X.: Hopf bifurcation analysis in a fluid flow model of internet congestion control algorithm. Nonlinear Anal. Real World Appl. **10**, 824–839 (2009)
23. Ding, D., Zhu, J., Luo, X., Liu, Y.: Controlling Hopf bifurcation in fluid flow model of Internet congestion control system. Int. J. Bifurc. Chaos **19**, 1415–1424 (2009)
24. Guo, S., Liao, X., Li, C.: Stability and Hopf bifurcation analysis in a novel congestion control model with communication delay. Nonlinear Anal. Real World Appl. **9**, 1292–1309 (2008)
25. Guo, S., Liao, X., Liu, Q., Li, C.: Necessary and sufficient conditions for Hopf bifurcation in exponential RED algorithm with communication delay. Nonlinear Anal. Real World Appl. **9**, 1768–1793 (2008)
26. Guo, S., Feng, G., Liao, X., Liu, Q.: Hopf bifurcation control in a congestion control model via dynamic delayed feedback. Chaos **18**, 043104 (2008)
27. Guo, S., Zheng, H., Liu, Q.: Hopf bifurcation analysis for congestion control with heterogeneous delays. Nonlinear Anal. Real World Appl. **11**, 3077–3090 (2010)
28. Hu, H., Huang, L.: Linear stability and Hopf bifurcation in an exponential RED algorithm model. Nonlinear Dyn. **59**, 463–475 (2010)
29. Liu, F., Guan, Z., Wang, H.: Stability and Hopf bifurcation analysis in a TCP fluid model. Nonlinear Anal. Real World Appl. **12**, 353–363 (2011)
30. Liu, F., Wang, H., Guan, Z.: Hopf bifurcation control in the XCP for the Internet congestion control system. Nonlinear Anal. Real World Appl. **13**, 1466–1479 (2012)
31. Rezaie, B., Jahed Motlagh, M.R., Khorsandi, S., Analoui, M.: Hopf bifurcation analysis on an Internet congestion control system of arbitrary dimension with communication delay. Nonlinear Anal. Real World Appl. **11**, 3842–3857 (2010)
32. Hale, J.: Theory of Functional Differential Equations. Springer, New York (1977)
33. Hassard, B., Kazarinoff, N., Wan, Y.: Theory and Applications of Hopf Bifurcation. Cambridge University Press, Cambridge (1981)
34. Nayfeh, A.H., Harb, A.M., Chin, C.M.: Bifurcations in a power system model. Int. J. Bifurc. Chaos **14**, 497–512 (1996)